

Electronic transitions in disk-shaped quantum dots induced by twisted light

G. F. Quinteiro and P. I. Tamborenea

Departamento de Física “Juan José Giambiagi,” Universidad de Buenos Aires, Ciudad Universitaria, Pabellón I, 1428 Ciudad de Buenos Aires, Argentina

(Received 22 October 2008; revised manuscript received 17 March 2009; published 30 April 2009)

We theoretically investigate the absorption and emission of light carrying orbital angular momentum (twisted light) by quasi-two-dimensional (disk-shaped) quantum dots in the presence of a static magnetic field. We calculate the transition matrix element for the light-matter interaction and use it to explore different scenarios, depending on the initial and final states of the electron undergoing the optically induced transition. We make explicit the selection rule for the conservation of the z projection of the orbital angular momentum. For a realistic set of parameters (quantum dot size, beam waist, photon energy, etc.) the strength of the transition induced by twisted light is 10% of that induced by plane waves. Finally, our analysis indicates that it may be possible to select precisely the electronic level one wishes to populate using the appropriate combination of light-beam parameters suggesting technological applications to the quantum control of electronic states in quantum dots.

DOI: [10.1103/PhysRevB.79.155450](https://doi.org/10.1103/PhysRevB.79.155450)

PACS number(s): 73.21.La, 78.20.Ci

I. INTRODUCTION

It is a common mathematical procedure to describe light as a superposition of plane waves, which is possible and convenient thanks to the linearity of Maxwell's equations and Fourier analysis. However, plane waves are only one of the possible *representations* of light, and despite its wide applicability, other representations may be better suited to tackle particular problems.¹ For example, the expansion of the field in multipolar waves is normally used to study the radiation associated with nuclei and atoms. Another less-known representation is the so-called twisted light (TL). As its name suggests, it has an helicoidal wave front that is mathematically introduced by a phase with azimuthal dependence, i.e., $e^{-il\phi}$, and a radial dependence of the *Laguerre-Gaussian* (LG) or *Bessel mode* type. A peculiarity of the TL representation is that all modes with same value of l have the same z projection of orbital angular momentum (OAM).

The recent development of techniques to generate coherent TL has boosted the study on many aspects of this peculiar type of radiation. Research involving TL has been done in numerous areas, such as generation of twisted beams,² interaction of OAM beams with mesoscopic particles (optical tweezers),³ entanglement between spin and OAM for potential applications to quantum-information science,⁴ interaction of OAM fields with atoms or molecules,⁵ and QED in confined geometries,⁶ with twisted beams. Nevertheless, the problem of the interaction of TL with condensed matter systems is largely unexplored;⁷ very recently we have presented the first study on the action of TL on a bulk semiconductor.⁸

Quantum dots (QDs) are well-studied man-made nanostructures.^{9,10} Different types of QDs, such as those produced by lateral confinement in a two-dimensional (2D) electron gas, vertical or stacked, nanowhisker-based, and self-assembled QDs, are available experimentally. They all share the basic feature of producing particle confinement in all directions, which gives rise to a discrete energy spectrum akin to that of atoms. Self-assembled, vertical, and nanowhisker QDs are fabricated using semiconductor materials,

and they can confine both electrons and holes. As the name suggests, disk-shaped quantum dots (DSQDs) have a stronger confinement along a given axis, and therefore the dynamics of electrons and/or holes inside the dot can be restricted to the quantized in-plane motion.¹¹ In semiconductor-based QDs, transitions between different electronic states can be accomplished by optical excitation. The understanding of the optical response of QDs is appealing from a basic science point of view but also because of the many possible applications, for example, to QD lasers, quantum-information processing, and photodetectors. In spite of the fact that the common Hermite-Gaussian laser pulses are widely used to excite QDs,¹² to the best of our knowledge, no work has been reported on the interaction of these nanostructures with twisted light.

Here we develop the theory of optical electronic transitions induced by TL in semiconductor-based DSQDs. We find the corresponding selection rule and discuss the use of TL as a versatile scheme to induce transitions that are not possible using common optical techniques. The article is organized as follows. In Sec. II we review the description of the TL electromagnetic field and of the electronic states of semiconductor-based DSQDs in the presence of an external magnetic field. Section III is devoted to the calculation of the matrix elements of the interaction Hamiltonian that couples the light field to the electrons in the DSQD; its applications to different cases are treated in Sec. IV. The special properties of the optical transitions induced by twisted light in QDs and possible technological applications become clear in this section. Finally, we summarize the results in Sec. V.

II. MODEL

For disk-shaped quantum dots, the electron's wave function can be written as the product of a microscopic cell-periodic function, an envelope function, and a spin part ξ , that is,

$$\psi(\mathbf{r}) = [\phi(r, \theta)Z(z)]u(\mathbf{r})\xi. \quad (1)$$

For the microscopic function $u(\mathbf{r})$, the strain in the QD lifts the degeneracy of the heavy-hole and light-hole bands; then,

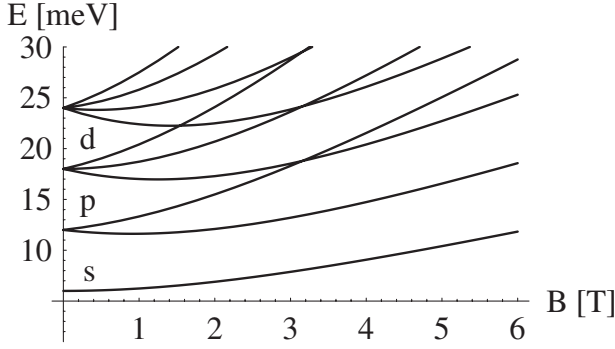


FIG. 1. Energy spectrum as a function of the magnetic field B for $\hbar\omega_0=6$ meV and $\hbar\omega_c=1.7B$ meV. The OAM of the envelope function is shown using the convention: $n=0(s)$, $n=1(p)$, $n=2(d)$, etc.

it is safe to restrict the study to a two-band model in the effective-mass approximation with a conduction and a heavy-hole bands. For the envelope function $[\phi(r, \theta)Z(z)]$, the disk shape of the QD allows for the separation into the vertical (z) and the in-plane (r, θ) motion. Furthermore, since the confinement in the z direction is much stronger than that in the x - y plane, it is a good approximation to assume that the electron remains in the lowest-energy z eigenstate. For DSQDs ranging in diameter from tens to a few hundreds of nanometers,^{11,13} the in-plane confinement potential can be well approximated by a two-dimensional harmonic oscillator potential $V_i(r) = \frac{1}{2}m_i^*\omega_{0i}^2r^2$, where $i=c, v$ denotes the conduction and valence bands and m_i^* is the effective electron mass. The corresponding single-particle problem with the inclusion of an external magnetic field B applied in the z axis is analytically solvable yielding eigenfunctions,¹⁴

$$\begin{aligned} \phi_{ism}(r, \theta) &= \frac{(-1)^s}{\sqrt{2\pi}\ell_i} \sqrt{\frac{s!}{(s+|n|)!}} e^{-r^2/(4\ell_i^2)} \left(\frac{r}{\sqrt{2}\ell_i}\right)^{|n|} L_s^{|n|} \\ &\times \left(\frac{r^2}{2\ell_i^2}\right) e^{-in\theta} = R_{ism}(r) e^{-in\theta}, \end{aligned} \quad (2)$$

where $\ell_i^2 = \hbar/(2|m_i^*\omega_i)$ is a characteristic length of the confinement of the electrons, $\omega_i^2 = \omega_{0i}^2 + \Omega_i^2/4$ with $\Omega_i = eB/(m_i^*c)$ the cyclotron frequency and $L_s^{|n|}$ is a generalized Laguerre polynomial with radial quantum number s and z projection of the OAM n . The energy spectrum of electrons in the conduction band is $E_c = \hbar\omega_c(2s+|n|+1) - (1/2)\hbar\Omega_c n$, while for electrons in the valence band it is $E_v = (\hbar\omega_{0c} - E_G) - [\hbar\omega_v(2s+|n|) - (1/2)\hbar\Omega_v n]$. In the presence of an external static magnetic field pointing in the z direction, the orbital degeneracy of the states is lifted, as shown in Fig. 1, and for strong enough fields the levels group into Landau levels (not shown in the figure).

Two different modes of TL beams are nowadays experimentally realizable, namely, the LG and the *Bessel* modes. We proceed to develop our theory for a general case, and in the final stages of the calculation we work with the LG modes in order to take advantage of the mathematical structure of the electronic wave functions given in Eq. (2), which contain the generalized Laguerre polynomials. In the

paraxial approximation, the vector potential of the TL beam is

$$\mathbf{A}(\mathbf{r}, t) = \epsilon F(\mathbf{r}) e^{i(kz - \omega t)} + \text{c.c.} = \mathbf{A}^{(+)}(\mathbf{r}, t) + \mathbf{A}^{(-)}(\mathbf{r}, t), \quad (3)$$

with ϵ the circular polarization vector normal to z and for the Laguerre-Gaussian modes

$$F(\mathbf{r}) = \left[\frac{C_p^{|l|}}{w_0} \left(\frac{\sqrt{2}r}{w_0}\right)^{|l|} e^{-r^2/w_0^2} L_p^{|l|} \left(\frac{2r^2}{w_0^2}\right) \right] e^{-il\theta} = F_r(r) e^{-il\theta}, \quad (4)$$

where w_0 is the beam waist, l is the z projection of the orbital angular momentum, and $C_p^{|l|}$ is a normalization constant.¹⁵

Our system, consisting of a single DSQD plus a TL light mode, is investigated using the semiclassical model where the light is treated classically and the electrons quantum mechanically. For the electron-light interaction we use the minimal-coupling Hamiltonian and calculate its optical-transition matrix elements using the eigenfunctions given in Eqs. (1) and (2). Since our main goal here is to explore the changes in the optical-transition selection rules brought about by the use of twisted light instead of plane waves, it is enough to work with a single-particle formalism. The influence of Coulomb electron-electron interaction, which causes excitonic effects, modification of the effective confining potential, etc., is left for future study.

III. TL OPTICAL DIPOLE MATRIX ELEMENTS

In order to determine the optical response, we calculate the matrix elements of the transitions induced by the light-matter Hamiltonian between single-particle states [Eq. (1)]. We use the minimal-coupling interaction and retain only the lowest order in the vector potential.¹⁶ This matrix element is the essential ingredient in many calculations, e.g., Fermi's golden rule for the rate of absorption/emission. To simplify the notation, we use as collective indices the Hebrew characters Aleph (\aleph) and Gimel (\beth) to replace the set $\{s, n, \xi\}$ [see Eqs. (1) and (2)], while the band index will still appear explicitly. The transition matrix element from an initial state $\{j, \beth\}$ to a final state $\{i, \aleph\}$ is

$$\begin{aligned} \langle i\aleph | H_I | j\beth \rangle &= -\frac{q}{m} \langle \psi_{i\aleph} | \mathbf{A}(\mathbf{r}) \cdot \mathbf{p} | \psi_{j\beth} \rangle \\ &= i\hbar \frac{q}{m} \int_{L^3} d^3r \psi_{i\aleph}^*(\mathbf{r}) \mathbf{A}(\mathbf{r}) \cdot \nabla \psi_{j\beth}(\mathbf{r}), \end{aligned}$$

where q is the charge ($-e$) and m is the bare electron mass. The operation $\nabla \psi_{j\beth}(\mathbf{r})$ yields three terms and we write

$$\begin{aligned}
\langle i\mathfrak{N}|H_I|j\mathfrak{L}\rangle &= i\hbar \frac{q}{m} \int_{L^3} d^3r u_i(\mathbf{r})^* u_j(\mathbf{r}) \mathbf{A}(\mathbf{r}) \cdot [\phi_{i\mathfrak{N}}(\mathbf{r})^* \nabla \phi_{j\mathfrak{L}}(\mathbf{r})] \\
&\times |Z(z)|^2 \xi_{\mathfrak{N}}^* \xi_{\mathfrak{L}} + i\hbar \frac{q}{m} \int_{L^3} d^3r \phi_{i\mathfrak{N}}(\mathbf{r})^* \phi_{j\mathfrak{L}}(\mathbf{r}) u_i(\mathbf{r})^* \\
&\times u_j(\mathbf{r}) \mathbf{A}(\mathbf{r}) \cdot [Z(z)^* \nabla Z(z)] \xi_{\mathfrak{N}}^* \xi_{\mathfrak{L}} + i\hbar \frac{q}{m} \\
&\times \int_{L^3} d^3r \phi_{i\mathfrak{N}}(\mathbf{r})^* \phi_{j\mathfrak{L}}(\mathbf{r}) \mathbf{A}(\mathbf{r}) \cdot [u_i(\mathbf{r})^* \nabla u_j(\mathbf{r})] \\
&\times |Z(z)|^2 \xi_{\mathfrak{N}}^* \xi_{\mathfrak{L}}. \quad (5)
\end{aligned}$$

The envelope functions and the vector potential are slowly varying and can be considered constant over a unit cell (lattice constant a); in contrast, the microscopic function $u(\mathbf{r})$ is periodic over unit cells. These two facts allow for the separation of the all-space integral (\int_{L^3}) into an intracell integral (\int_{a^3}) and an intercell sum (\sum_c).¹⁷ Due to the orthogonality of the microscopic function in a cell, the first and second terms in the sum are nonzero only for intraband transitions (notice also that the second one represents inter- z -band transitions, which are unlikely under strong confinement in the z direction). As we are interested in optical-frequency transitions which correspond to interband transitions, we focus our attention on the last term

$$\begin{aligned}
\langle i\mathfrak{N}|H_I|j\mathfrak{L}\rangle &= \frac{-q}{m} \xi_{\mathfrak{N}}^* \xi_{\mathfrak{L}} \left[\int_{a^3} d^3r u_i(\mathbf{r})^* (-i\hbar \nabla) u_j(\mathbf{r}) \right] \\
&\cdot \left[\sum_c \phi_{i\mathfrak{N}}(\mathbf{r}_c)^* \phi_{j\mathfrak{L}}(\mathbf{r}_c) |Z(z_c)|^2 \mathbf{A}(\mathbf{r}_c) \right], \quad (6)
\end{aligned}$$

which is simplified by taking the continuum limit, thus transforming the sum over cells to an intercell integral according to $\Sigma \rightarrow (1/a^3)\int$, and defining the matrix element $a^3 \mathbf{p}_{ij} = \int_{a^3} d^3r u_i(\mathbf{r})^* (-i\hbar \nabla) u_j(\mathbf{r})$. The vector potential [Eq. (3)] consists of two terms. Inserting the positive part $\mathbf{A}^{(+)}(\mathbf{r}, t)$ in Eq. (6),

$$\begin{aligned}
\langle i\mathfrak{N}|H_I^{(+)}|j\mathfrak{L}\rangle &= -e^{-i\omega t} \frac{2\pi q}{m} (\boldsymbol{\epsilon} \cdot \mathbf{p}_{ij}) \delta_{l, (n_{\mathfrak{N}} - n_{\mathfrak{L}})} \\
&\times \delta_{\xi_{\mathfrak{N}}, \xi_{\mathfrak{L}}} \int_0^\infty dr r F_r(r) R_{i\mathfrak{N}}(r)^* R_{j\mathfrak{L}}(r), \quad (7)
\end{aligned}$$

where l corresponds to the vector potential and n to the wave functions, and we assumed that the light's wavelength is much larger than the QD's height so that $e^{ikz} \simeq 1$.

The matrix element $\langle i\mathfrak{N}|H_I^{(+)}|j\mathfrak{L}\rangle$ contains two terms which represent valence-to-conduction and conduction-to-valence band transitions, respectively. We eliminate one of them by using the rotating-wave approximation (RWA) and obtain

$$\begin{aligned}
\langle c\mathfrak{N}|H_I^{(+)}|v\mathfrak{L}\rangle &= -e^{-i\omega t} \frac{2\pi q}{m} (\boldsymbol{\epsilon} \cdot \mathbf{p}_{cv}) \delta_{l, (n_{\mathfrak{N}} - n_{\mathfrak{L}})} \delta_{\xi_{\mathfrak{N}}, \xi_{\mathfrak{L}}} \\
&\times \int_0^\infty dr r F_r(r) R_{c\mathfrak{N}}(r)^* R_{v\mathfrak{L}}(r) \quad (8)
\end{aligned}$$

for the absorption of light. The same can be done with $\mathbf{A}^{(-)}(\mathbf{r}, t)$ yielding

$$\begin{aligned}
\langle v\mathfrak{N}|H_I^{(-)}|c\mathfrak{L}\rangle &= -e^{i\omega t} \frac{2\pi q}{m} (\boldsymbol{\epsilon}^* \cdot \mathbf{p}_{vc}) \delta_{l, (n_{\mathfrak{L}} - n_{\mathfrak{N}})} \delta_{\xi_{\mathfrak{N}}, \xi_{\mathfrak{L}}} \\
&\times \int_0^\infty dr r F_r(r) R_{v\mathfrak{N}}(r)^* R_{c\mathfrak{L}}(r) \quad (9)
\end{aligned}$$

for the emission of light. Further simplification and analysis of Eqs. (8) and (9) are only possible once specific functions $F_r(r)$, $R_{v\mathfrak{N}}(r)$, and $R_{v\mathfrak{L}}(r)$ are given. This will be done in Sec. IV.

Note that the selection rule for the conservation of the z component of the OAM in the system of electron plus light field appears explicitly in Eqs. (8) and (9). For absorption and emission processes we get $\delta_{l, (n_{\mathfrak{N}} - n_{\mathfrak{L}})}$ and $\delta_{l, (n_{\mathfrak{L}} - n_{\mathfrak{N}})}$, respectively.

IV. TL-INDUCED OPTICAL TRANSITIONS

The theory developed in Sec. III will be used here to study specific cases of optical transitions between QD levels in order to get a firmer insight into the possibilities opened by excitation with twisted light. An important goal is to determine how the beam parameters $\{p, l\}$ [see Eq. (4)] enable us to choose the allowed transitions and their strength. In what follows we will study the excitation process for the case of Laguerre-Gaussian beams. Then the matrix element of $H_I^{(-)}$ between initial and final states yields zero. From Eq. (8) with $\mathfrak{L} = (sn\alpha)$ and $\mathfrak{N} = (tm\beta)$, after inserting the expressions for $R(r)$ and $F_r(r)$, rearranging terms, and transforming coordinates to $x = r^2 / (2\ell_c^2)$, we obtain

$$\begin{aligned}
\langle c\mathfrak{N}|H_I^{(+)}|v\mathfrak{L}\rangle &= -e^{-i\omega t} \frac{2\pi q}{m} (\boldsymbol{\epsilon} \cdot \mathbf{p}_{cv}) \delta_{\alpha, \beta} \delta_{l, (m-n)} \frac{C_p^{|l|}}{w_0} \frac{(-1)^{s+t}}{2\pi} \\
&\times \sqrt{\frac{t! s!}{(t+|m|)! (s+|n|)!}} \xi^{|l|/2} \int_0^\infty dx x^{(|n|+|m|+|l|)/2} e^{-x(1+\zeta/2)} L_p^{|l|}(\xi x) L_t^{|m|}(x) L_s^{|n|}(x), \quad (10)
\end{aligned}$$

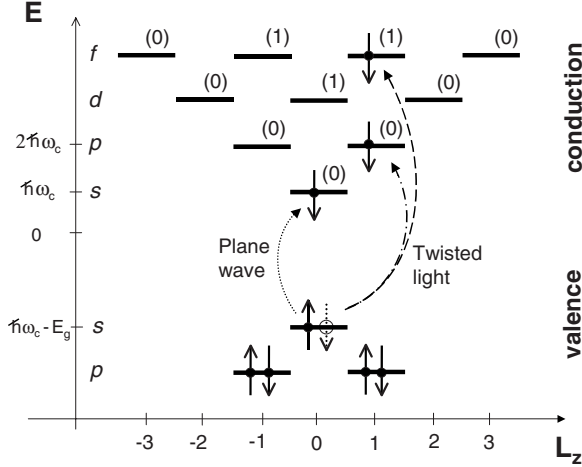


FIG. 2. Schematic representation of the single-particle levels and optical transitions for zero magnetic field: an electron with spin down has been promoted from a valence-band state to a conduction-band state. The transition induced by plane waves (dotted line) can only be “vertical” while transitions induced by twisted light (dash-dotted and dashed lines) need not be vertical but must obey the selection rule for the z component of OAM; we show the transition for light-carrying OAM $l=1$. The convention of Eq. (2) is adopted for electronic states: $L_z=n$ and the number between parenthesis is the radial quantum number s . The shells are given by the letters $\{s, p, d, \dots\}$ as customary in atomic physics.

where we assumed that $\ell_c = \ell_v$ (Ref. 18) and defined $\zeta = 4\ell_c^2/w_0^2$.

Working with Eq. (10), in Sec. IV A we analyze the optical transitions induced by twisted light from the uppermost valence-band state ($s=n=0$) to a general state in the conduction band (see Fig. 2). This case offers the mathematical advantage of having only two generalized Laguerre polynomials in the integral of Eq. (10), enabling the use of their orthogonality relations in order to go farther with the analytical treatment of the matrix elements. We concentrate on the physically relevant case of small QDs (small compared to the size of the beam’s waist) in which the parabolic approximation for the confinement potential is best suited. For small dots, we compare the strength of the transitions induced by twisted light with that of the transitions induced by plane waves. This is done by considering the particular case of a beam without OAM [$l=0$ in Eq. (10)], which resembles plane-wave light. In Sec. IV B we extend the analysis by solving numerically Eq. (10) for a general valence-band initial state and for any relative sizes of QD and beam waist. Finally, in Sec. IV C we discuss some of the possibilities opened by the use of TL in optical excitation experiments from the point of view of quantum control of the electronic states in QDs.

A. Transitions from uppermost valence-band state

Let us consider a QD in its ground state, i.e., with all electrons occupying the valence-band levels. The transition of an electron from the valence-band uppermost state to an arbitrary unoccupied state in the conduction band will be

shown to be possible by choosing the appropriate beam parameters. The electron in its initial state has wave function $\psi_{v00\beta}(\mathbf{r}) = R_{v00}(r)\beta$ with $R_{v00}(r) = (\sqrt{2\pi}\ell_v)^{-1}\exp[-r^2/(4\ell_v^2)]$, while the final excited state is $\psi_{c sn\alpha}(\mathbf{r})$ [see Eq. (2)]. From Eq. (10) with $\aleph = (sn\alpha)$ and $\lambda = (00\beta)$ we arrive at

$$\langle c\aleph | H_I^{(+)} | v\lambda \rangle = -\frac{C_p^{|l|}}{w_0} (-1)^s \sqrt{\frac{s!}{(s+|l|)!}} \times e^{-i\omega t} \frac{q}{m} (\boldsymbol{\epsilon} \cdot \mathbf{p}_{cv}) \delta_{\alpha,\beta} \delta_{l,n} h(\zeta), \quad (11)$$

where the dimensionless function $h(\zeta)$ is

$$h(\zeta) = \zeta^{l/2} \int_0^\infty dx x^{|l|} e^{-x(1+\zeta/2)} L_p^{|l|}(\zeta x) L_s^{l|}(x). \quad (12)$$

For QDs with sizes ranging from 10 to 200 nm, together with the minimum size of the beam waist $w_0=500$ nm, we obtain $0.001 < \zeta < 0.6$. Thus, it is reasonable to keep in Eq. (12) only the lowest orders in ζ . Without loss of generality, we assume $l \geq 0$. We simplify the integral in Eq. (12) with the help of Eq. (A2) to reduce $L_p^l(\zeta x)$. Thus, we write $h(\zeta) = \zeta^{l/2}(I_0 + I_1 + \dots)$, with

$$I_0 = \frac{(l+p)!}{p!} \delta_{0s},$$

$$I_1 = \zeta \frac{(l+p)!}{p!} \left(p + \frac{l+1}{2} \right) (\delta_{1s} - \delta_{0s}), \quad (13)$$

where the integral $\int_0^\infty dx x^l e^{-x} x L_0^l(x) L_s^l(x)$ was reduced by using Eq. (A3) and the fact that $L_0^l(x)=1$ so $x L_0^l(x) L_s^l(x) = [(1+l)L_0^l(x) - L_1^l(x)] L_s^l(x)$.

Let us now verify that a “twisted-light” beam without OAM ($l=0$) yields the same result as plane-wave light. For small QDs, we obtain from Eq. (13) $I_0 + I_1 = (1-\zeta/2)\delta_{0j} + \zeta/2\delta_{1j}$, but since an ideal plane wave has $\zeta \rightarrow 0$ we keep only the zeroth-order term in ζ in this expression. If we focus on the lowest-energy transition ($v00\alpha \Rightarrow c00\alpha$) we obtain

$$H_I^{(+)}|_{\text{PW}} \simeq -e^{-i\omega t} \frac{C_0^0}{w_0} \frac{q}{m} (\boldsymbol{\epsilon} \cdot \mathbf{p}_{cv}); \quad (14)$$

this transition, which we named here PW, is depicted in Fig. 2 as a dotted line labeled “plane wave.” The coefficient C_0^0/w_0 is the amplitude of the vector potential. Note that the plane-wave limit is obtained by taking $w_0 \rightarrow \infty$ and $C_0^0 \rightarrow \infty$ simultaneously, keeping the ratio constant.

We can now compare the relative strength of transitions induced by the usual PW light and twisted light for small QDs. In Fig. 2, TL transitions are shown as dash-dotted and dashed lines labeled “twisted light” for the particular value of $l=1$. Retaining the lowest order in ζ in Eq. (13) also for the TL mode, we obtain the ratio of amplitudes

$$\left| \frac{H_I^{(+)}|_{\text{TL}}}{H_I^{(+)}|_{\text{PW}}} \right| = \frac{C_p^l}{C_0^0} \sqrt{\frac{s!}{(s+l)!}} \frac{(l+p)!}{p!} \zeta^{l/2}. \quad (15)$$

Notice the power-law dependence on ζ , with exponent $l/2$. For small QDs (i.e., small ζ), the transition amplitude with

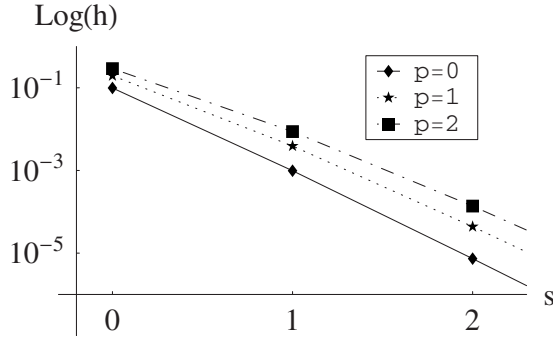


FIG. 3. Strength of the optical-transition from uppermost valence-band state: logarithm of the dimensionless function $h(\zeta)$ [Eq. (12)] as a function of the radial quantum number s of the final electronic state for $\zeta=0.01$ and beam parameters $l=1$ and $p=0,1,2$. For this small value of ζ the TL-induced excitation is dominated by the transition from the state $\lambda=(00\beta)$ in the valence band to the state $\aleph=(s2\beta)$ with $s=0$ in the conduction band; the transition amplitudes to states with $s \neq 0$ are several orders of magnitude smaller.

TL becomes weaker in comparison to that of PW light as the OAM of the light beam increases. We expect Eq. (15) to be helpful in future experiments on optical transitions with TL since it is cast as a comparison with the standard optical transitions.

Lastly, let us examine the role of the radial quantum number of the final state. Still considering small dots, Eq. (13) suggests that transitions to all values of the final radial quantum number s are allowed and have amplitudes on the order of $\zeta^{s+l/2}$ [shown in Eq. (13) up to an order of 1]. Figure 3 displays the strength, given by the function $h(\zeta)$ of Eq. (12), of the transitions to final states with $s=0,1,2$, calculated numerically to all orders in ζ for $l=1$. Two of these transitions are illustrated in Fig. 2: the zeroth-order one shown as a dash-dotted line and the first-order one as a dashed line. In Fig. 3 we choose $\zeta=0.01$. For this small value of ζ the TL-induced excitation is dominated by the transition from the valence-band state $\lambda=(00\beta)$ to the conduction-band state $\aleph=(s2\beta)$ with $s=0$. There is a strong dependence on s , and it can be seen that the transition amplitudes to states with $s \neq 0$ are several orders of magnitude smaller. We will see in Sec. V that this situation changes radically for QDs and beam waists of comparable sizes.

B. Transitions from general valence-band state

Here we consider the transition of an electron initially in a general valence-band state $\psi_{v\lambda}(\mathbf{r})$ to a conduction-band state $\psi_{c\aleph}(\mathbf{r})$, with collective indices $\lambda=(sn\alpha)$ and $\aleph=(tm\beta)$. The analytical solution of the integral appearing in Eq. (10), although possible, is cumbersome (see Appendix B). Therefore, we present numerical results for the function

$$h(\zeta) = \zeta^{l/2} \int_0^\infty dx x^{(|n|+|m|+|l|)/2} e^{-x(1+\zeta/2)} \times L_p^{|l|}(\zeta x) L_t^{|m|}(x) L_s^{|n|}(x), \quad (16)$$

which allow us to explore all values of ζ . A value of $\zeta > 1$

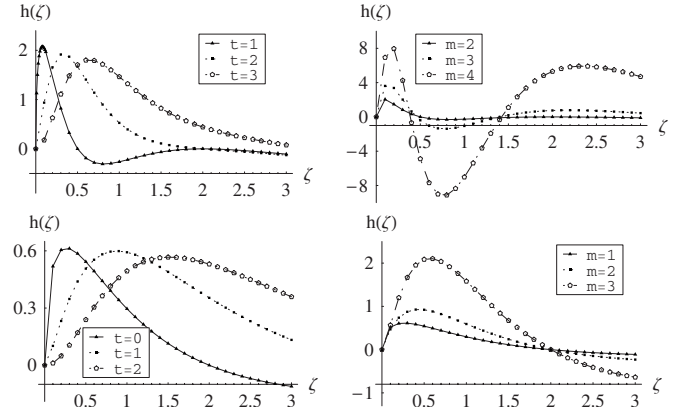


FIG. 4. Strength of the optical transition from general valence-band states: dimensionless function $h(\zeta)$ [Eq. (16)]. Light parameter $p=1$ in all cases. Top left: from state $(s=1, n=1)$ to $(t, m=2)$. Top right: from state $(s=1, n=1)$ to $(t=1, m)$. Bottom left: from state $(s=0, n=0)$ to $(t, m=1)$. Bottom right: from state $(s=0, n=0)$ to $(t=0, m)$. Transitions from the same initial state are displayed on the same row. Curves on the left column represent transitions to final states with varying radial quantum number t . Curves on the right column represent transitions to final states with varying z projection of the OAM m .

represents a situation of a narrow beam interacting with a large structure. Even though the parabolic approximation for the confining potential is likely not to be valid for quantum disks of such sizes, our calculation may provide qualitatively correct results.

In Fig. 4 we plot $h(\zeta)$ from Eq. (16). We consider two different initial states. The bottom row corresponds to transitions from the uppermost valence-band state, and it is thus an extension of the results of Sec. III to general values of ζ . On the bottom-left panel we plot three possible transitions to final states differing only in their radial quantum number t . Pictorially, these states would lie, in Fig. 2, on a vertical line. We see that for values of ζ up to about 0.5 (small QDs) the transition to the final state with $s=0$ is the dominant one, which is consistent with the analytical results of Sec. III for $\zeta \approx 0$. With increasing ζ the relative strength of the three transitions is altered, and for $\zeta > 1.4$ the order of the three transitions is inverted compared to the situation at $\zeta < 0.5$. The bottom-right panel shows transitions to final states with varying z projection of the OAM for fixed radial quantum number $t=0$. These transitions can be visualized in Fig. 2 as having final states lying on the lowest diagonal going up and to the right. The top row of Fig. 4 presents analogous results but for transitions originating in the valence-band state ($s=1, n=1$), chosen somewhat arbitrarily to illustrate the more general case. Besides a change in scale from top to bottom panels, the similarities among them are obvious.

We briefly comment on the relative strength of transitions induced by plane waves and those induced by TL, as done in Sec. IV A [see Eq. (15)], but now for the case of an arbitrary initial state. For $\zeta \rightarrow 0$ we note that the integral in $h(\zeta)$ tends to a constant (see Appendix B) and we recover the result of $h(\zeta) \propto \zeta^{l/2}$. On the other hand, we cannot give a simple expression for the ratio of transition strengths for large ζ , and the actual dependence on ζ must be found by solving the integral in Eq. (16).

C. Manipulation of electronic states

Our study suggests that twisted light is a versatile tool to optically manipulate states in QDs. By a smart choice of beam parameters, QD size, and external static magnetic field one can select precisely the electronic level to be populated. In the following, we illustrate, with two examples, how this can be accomplished.

Let us assume that we wish to connect the uppermost valence-band state with the f -shell conduction-band state ($n=1$, $s=1$) [see Eq. (2)] on a small QD ($\zeta \ll 1$); this transition is depicted as a dashed line in Fig. 2. We first choose the light-beam parameters: tune the laser on resonance (or close) with the energy difference between these states ($\Delta E = E_g + 3\hbar\omega_c$) and take $l=1$ and $p=0$ (from our previous analysis, the value of p is not very important). With this requirements, not only the desired transition is possible but also another one that promotes an electron from the p -shell valence-band state ($n=-1$, $s=0$) to the d -shell conduction-band state ($n=1$, $s=0$). Nevertheless, if a static magnetic field is applied, one of these transitions can be moved off resonance from the light (see in Sec. II the general expressions for the energy levels with magnetic field), leaving only one dominant transition.

For our second example we will assume that the laser cannot be tuned precisely to match the energy difference between a couple of states and that we deal with a QD of larger size of, say, about 400 nm. This last assumption means that, by modifying the light-beam waist, we can choose ζ on the interval (0,1). Then, by selecting the light-beam parameter l we instantly eliminate transitions between states differing more than l in their z projection of OAM. Furthermore, by adjusting the beam waist, we see that we can change the probability of transition depending on the value of the radial quantum number of the electronic states (see Fig. 4). To fix ideas, let us imagine that the emission line of the light beam is centered around $E_g + 2\hbar\omega_c$ with width $\hbar\omega_c$. Under these conditions, transitions from the uppermost valence-band state to shells p, d, f in the conduction band are possible. If we choose beam parameters $l=1$ and $p=0$, and waist such that $\zeta \approx 1$ the dominant transition will become that to the f -shell conduction-band state ($t=1, m=1$). Thus, we conclude that even if the laser cannot be precisely tuned, we still can decide which will be the dominant transitions.

V. CONCLUDING REMARKS

We have investigated the theory of optical absorption of twisted light—carrying orbital angular momentum—by disk-shaped semiconductor-based quantum dots in the presence of a static magnetic field and calculated the dipole transition matrix element, which is the basic building block for other specific studies of optical response.

As a first general result we made explicit the selection rule for the conservation of the z projection of the orbital angular momentum. In addition, we observe that not only vertical but also more general transitions are possible, due to the fact that the z component of the orbital angular momentum of a TL beam can assume any integer value.

Different scenarios were explored according to what the initial and final states of the electron in the QD are. In the first place, we studied the transitions of an electron from the uppermost valence-band state to any conduction-band states and obtained analytical expressions in terms of powers of the ratio ζ of the QD size to the light-beam waist. For realistic values of ζ the strength of the transition induced by TL can be around 10% of the value of the transition using common laser (nontwisted) fields. We also considered the transitions that bring an electron from any valence-band states to any conduction-band states. This case was studied for larger values of ζ , and it enabled us to qualitatively think of the physics of similar systems, such as large QDs or quantum disks. Finally, we found that ζ plays also a role in selecting the most likely transitions. In all scenarios, we found that a smart choice of beam parameters (z projection of OAM, radial quantum number, energy, and beam waist) allows one to select which state the electron will be promoted to.

The current availability of sources of coherent beams of TL permits us to envisage their use for more versatile quantum control of electronic states in QDs and the indirect control of magnetization in doped QDs. Our theoretical analysis suggests that it may be possible to select precisely the electronic level one wishes to populate using the appropriate combination of beam parameters (and nanostructure size). In particular, derived formulas and results for ζ around 0.1 are directly applicable to disk-shaped semiconductor-based quantum dots; therefore, our predictions may be experimentally verified using current technology.

We have left unexplored the interesting issue of the generation of local nanometric-scale magnetic fields. It should be clear that—although this effect may be small—the absorption of twisted-light photons entails a transfer of OAM to the system with the resulting emergence of an electronic current within the QD, which in turn produces a magnetic field.⁸

ACKNOWLEDGMENTS

We are grateful to Pawel Hawrylak for useful discussions. We acknowledge support through ANPCyT (Grant No. PICT-2006-02134), CONICET (Grant No. PIP 5851), and UBACyT (Grant No. X495). G.F.Q. also acknowledges support from the National Research Council of Canada (Ottawa). P.I.T. is a researcher of CONICET.

APPENDIX A: LAGUERRE POLYNOMIALS

The Laguerre polynomials verify the following identities. The orthogonality condition

$$\int_0^\infty e^{-x} x^\alpha L_n^\alpha(x) L_m^\alpha(x) dx = \frac{\Gamma(n+\alpha+1)}{n!} \delta_{nm}, \quad (\text{A1})$$

the relation

$$L_m^\beta(\tau x) = \sum_{n=0}^{\infty} \binom{\beta+m}{m-n} \tau^n (1-\tau)^{m-n} L_n^\beta(x) \\ \simeq \binom{\beta+m}{m} (1-m\tau) L_0^\beta(x) + \binom{\beta+m}{m-1} \tau L_1^\beta(x) \quad (\text{A2})$$

from Niukkanen,¹⁹ and the second line is for $\tau \rightarrow 0$. Also,

$$x = (1+l)L_0^l(x) - L_1^l(x) \quad (\text{A3})$$

and

$$L_m^\beta(x) = \sum_n \frac{(\beta-\alpha)_{m-n}}{(m-n)!} L_n^\alpha(x), \quad (\text{A4})$$

where $(a)_i = \Gamma(a+i)/\Gamma(a)$ is a Pochhammer symbol. Finally

$$L_m^k(x) L_n^l(x) = \sum_{\alpha=0}^{\infty} (-1)^\alpha D_\alpha L_{m+n-\alpha}^{k+l}(x). \quad (\text{A5})$$

APPENDIX B: ANALYTICAL SOLUTION FOR ANY-TO-ANY TRANSITION

Without loss of generality, we make $l, n, m > 0$ in Eq. (16),

$$h(\zeta) = \xi^{l/2} \int_0^\infty dx x^m e^{-x(1+\zeta/2)} L_p^{m-n}(\zeta x) L_t^m(x) L_s^n(x), \quad (\text{B1})$$

and solve the integral, for small ζ , using Eqs. (A2) and (A4), and $L_0^{n-m}(x) = 1$. Writing $h(\zeta) = \zeta^{l/2}(I_0 + I_1 + \dots)$ in orders of ζ ,

$$I_0 = \binom{m-n+p}{p} \frac{(n-m)_{s-t}}{(s-t)!} \frac{\Gamma(t+m+1)}{t!},$$

$$I_1 = \zeta \binom{l+p}{p} \frac{(n-m)_{s-t}}{(s-t)!} \frac{\Gamma(t+m+1)}{t!} \left(\frac{1+l}{2} - p \right) + \zeta \left[\binom{l+p}{p-1} + \frac{1}{2} \binom{l+p}{p} \right] I_{11}, \quad (\text{B2})$$

where $(a)_i = \Gamma(a+i)/\Gamma(a)$ is a Pochhammer symbol and $I_{11} = \int_0^\infty dx x^m e^{-x} L_1^l(x) L_t^m(x) L_s^n(x)$ can be formally reduced using Eq. (A5).

Equation (B1) admits also a simple solution for the particular case of $p=0$, following the same reasoning as done in Sec. IV A.

- ¹S. J. Van Enk and G. Nienhuis, *J. Mod. Opt.* **41**, 963 (1994).
- ²M. Padgett, J. Courtial, and L. Allen, *Phys. Today* **57**(5), 35 (2004).
- ³S. Barreiro and J. W. R. Tabosa, *Phys. Rev. Lett.* **90**, 133001 (2003); B. Allen, *J. Opt. B: Quantum Semiclassical Opt.* **4**, S1 (2002); M. E. J. Friese, T. A. Nieminen, N. R. Heckenberg, and H. Rubinsztein-Dunlop, *Nature (London)* **394**, 348 (1998).
- ⁴B. A. Muthukrishnan and C. R. Stroud, Jr., *J. Opt. B: Quantum Semiclassical Opt.* **4**, S73 (2002).
- ⁵B. L. C. Dávila Romero, D. L. Andrews, and M. Babiker, *J. Opt. B: Quantum Semiclassical Opt.* **4**, S66, (2002); F. Araoka, T. Verbiest, K. Clays, and A. Persoons, *Phys. Rev. A* **71**, 055401 (2005).
- ⁶S. Al-Awfi and M. Babiker, *Phys. Rev. A* **61**, 033401 (2000).
- ⁷T. P. Simula, N. Nygaard, S. X. Hu, L. A. Collins, B. I. Schneider, and K. Mølmer, *Phys. Rev. A* **77**, 015401 (2008).
- ⁸G. F. Quinteiro and P. I. Tamborenea, *EPL* **85**, 47001 (2009).
- ⁹S. M. Reimann and M. Manninen, *Rev. Mod. Phys.* **74**, 1283 (2002).
- ¹⁰L. Jacak, P. Hawrylak, and A. Wójs, *Quantum Dots* (Springer-Verlag, Berlin, 1998).
- ¹¹K. Brunner, U. Bockelmann, G. Abstreiter, M. Walther, G. Böhm, G. Trankle, and G. Weimann, *Phys. Rev. Lett.* **69**, 3216 (1992); S. Tarucha, D. G. Austing, T. Honda, R. J. van der Hage, and L. P. Kouwenhoven, *ibid.* **77**, 3613 (1996); M. A. Reed, J.

- N. Randall, R. J. Aggarwal, R. J. Matyi, T. M. Moore, and A. E. Wetsel, *ibid.* **60**, 535 (1988); P. M. Petroff, A. Lorke, and A. Imamoglu, *Phys. Today* **54**, 46 (2001).
- ¹²P. Hawrylak, G. A. Narvaez, M. Bayer, and A. Forchel, *Phys. Rev. Lett.* **85**, 389 (2000).
- ¹³M. Bayer, A. Schmidt, A. Forchel, F. Faller, T. L. Reinecke, P. A. Knipp, A. A. Dremin, and V. D. Kulakovskii, *Phys. Rev. Lett.* **74**, 3439 (1995).
- ¹⁴V. D. Granados and N. Aquino, *J. Mol. Struct.: THEOCHEM* **493**, 37 (1999).
- ¹⁵B. L. C. Dávila-Romero, D. L. Andrews, and M. Babiker, *J. Opt. B: Quantum Semiclassical Opt.* **4**, S66 (2002).
- ¹⁶The vector potential in the LG mode is *not* expressed in the Coulomb gauge; then, the minimal-coupling Hamiltonian $1/(2m)(\mathbf{p}-q\mathbf{A})^2$ yields an extra term: $(\mathbf{p}\cdot\mathbf{A})$ where it is understood that the momentum operator only acts upon the vector potential. This term need not be considered in our analysis since it does not contribute to interband transitions.
- ¹⁷Harmut Haug and Stephan W. Koch, *Quantum Theory of the Optical and Electronic Properties of Semiconductors*, 2nd ed. (World Scientific, Singapore, 1993), Chap. 5.
- ¹⁸S. Raymond, S. Studenikin, A. Sachrajda, Z. Wasilewski, S. J. Cheng, W. Sheng, P. Hawrylak, A. Babinski, M. Potemski, G. Ortner, and M. Bayer, *Phys. Rev. Lett.* **92**, 187402 (2004).
- ¹⁹A. W. Niukkanen, *J. Phys. A* **18**, 1399 (1985).